NeuroImage 197 (2019) 191–199

Contents lists available at ScienceDirect

NeuroImage

journal homepage: www.elsevier.com/locate/neuroimage

Structural connectivity prior to whole-body sensorimotor skill learning associates with changes in resting state functional connectivity

Nobuaki Mizuguchi [a,b,c], Tom Maudrich [a,d], Rouven Kenville [a,d], Daniel Carius [d], Dennis Maudrich [a], Arno Villringer [a,e,f], Patrick Ragert [a,d,*]

[a] Department of Neurology, Max Planck Institute for Human Cognitive and Brain Sciences, Leipzig, 04103, Germany
[b] Faculty of Science and Technology, Keio University, 3-14-1 Hiyoshi, Kohoku-ku, Yokohama, Kanagawa, 223-8522, Japan
[c] The Japan Society for the Promotion of Science, 5-3-1 Kojimachi, Chiyoda-ku, Tokyo, 102-0083, Japan
[d] Institute for General Kinesiology and Exercise Science, Faculty of Sport Science, University of Leipzig, Leipzig, 04109, Germany
[e] Clinic for Cognitive Neurology, University of Leipzig, Leipzig, 04103, Germany
[f] Berlin School of Mind and Brain, Mind and Brain Institute, Berlin, 10099, Germany

ARTICLE INFO

Keywords:
Serial reaction time task
Resting state functional connectivity
Fixel-based analysis
Prefrontal cortex
Striatum
Motor skill

ABSTRACT

Changes in resting state functional connectivity are induced by sensorimotor training and assumed to be concomitant of motor learning, although a potential relationship between functional and structural connectivity associated with sensorimotor sequence learning remains elusive. To investigate whether initial structural connectivity relates to changes in functional connectivity, we evaluated resting state functional connectivity (rs-FC), white matter fibre density (FD), fibre-bundle cross-section (FC), and gray matter volume (GMV) in healthy human participants before and after two days of performing a complex whole-body serial reaction time task (CWB-SRTT). As CWB-SRTT was implicit, participants were not told about the presence of any sequence. Since the lateral prefrontal cortex (PFC) plays an important role in sequence learning, we hypothesized that structural connectivity within the PFC prior to learning is associated with changes in rs-FC involving the lateral PFC. Sequence specific improvements, as assessed by the time difference between the last random and the last sequence blocks, were observed for reaction times, suggesting that sensorimotor sequence memory was acquired. Rs-FC between the right lateral PFC and bilateral striatum increased significantly in the learning group, when compared to a control group who performed only random blocks. This indicated that rs-FC changes are related to sequence memory but not to exercise itself. In addition, changes in rs-FC between the right lateral PFC and the left striatum were correlated with sequence specific improvements in individual reaction times. Furthermore, changes in rs-FC between right lateral PFC and left striatum were positively correlated with FC in the right anterior corona radiata measured before the task. We did not find any structural changes or significant correlations in FD or GMV. These findings suggest that an early phase of sensorimotor sequence learning in complex whole-body movements is associated with an increase in rs-FC between prefrontal and subcortical regions. Furthermore, we provide novel evidence that CWB-SRTT-induced changes in rs-FC were correlated with FC within the PFC.

1. Introduction

Motor skill learning is essential for various aspects such as physical education, neural rehabilitation, and sports. Until now, stationary serial reaction time tasks (SRTT) using upper limbs were often utilized to investigate neural substrates in association with sensorimotor sequence learning (Robertson, 2007). Previous studies have shown numerous brain areas to be involved in the development of sensorimotor sequence memory, namely prefrontal cortex (PFC), parietal cortex, supplementary motor area, primary motor cortex (M1), striatum and cerebellum (Schendan et al., 2003; Lehéricy et al., 2005; Dayan and Cohen, 2011). In this context, it could be demonstrated that such SRTT induced changes in resting state functional connectivity (rs-FC) such as fronto-parietal and sensorimotor networks immediately after the task, with these changes remaining for several hours (Sami et al., 2014). This suggests that learning-induced changes in rs-FC likely reflect offline learning. It has been shown that offline gains following sensorimotor sequence learning were also associated with white matter microstructure within the PFC

* Corresponding author. Institute for General Kinesiology and Exercise Science, Faculty of Sport Science, University of Leipzig, Leipzig, 04109, Germany.
E-mail address: patrick.ragert@uni-leipzig.de (P. Ragert).

https://doi.org/10.1016/j.neuroimage.2019.04.062
Received 29 November 2018; Received in revised form 12 April 2019; Accepted 23 April 2019
Available online 25 April 2019

(Vien et al., 2016). Furthermore, recent imaging studies suggest that rs-FC is influenced by individual anatomical structures or connectivity (Betzel et al., 2014; Ruddy et al., 2017). For example, changes in rs-FC with ageing were associated with a decrease in the density and weight in wider range of anatomical white-matter connections (Betzel et al., 2014). However, a potential relationship between initial structural connectivity and learning-induced changes in functional connectivity remains elusive. Therefore, multi-modal brain assessments immediately before and after sensorimotor sequence learning, through the inclusion of functional and structural measurements, would promote a better understanding of the respective neural mechanisms.

Although differences in brain activity during complex whole-body movements and easy hand movements are evident (Mizuguchi et al., 2016, 2018; Mizuguchi and Kanosue, 2017), functional and anatomical connectivity in association with sensorimotor sequence learning of complex whole-body movements remain to be examined. Indeed, whole body movements pose additional requirements regarding motor control such as interlimb coordination and postural control when compared to simple hand movements. Therefore, it is reasonable to assume that neural substrates of sensorimotor sequence learning differ between whole-body and simple hand movements. Since learning complex whole-body movements is an essential prerequisite for high performance levels in competitive sports and physical demands in everyday life, a better characterization of neural changes associated with the acquisition of such complex movement patterns is a crucial step for optimizing current training regimes. To investigate this, we modified a standard SRTT paradigm, so it could be performed using the lower extremities. Here, we evaluated rs-FC, white matter structure and gray matter volume (GMV) before and after two days of complex whole-body SRTT (CWB-SRTT). A previous study using functional magnetic-resonance imaging (MRI) demonstrated that both declarative/explicit and implicit sensorimotor sequence memory are potentially located in the lateral PFC (Schendan et al., 2003). In addition, studies involving virtual lesion approaches and patients with brain lesions suggested that the lateral PFC plays a substantial role in sequence learning (Gómez Beldarrain et al., 1999; Robertson et al., 2001; Schmidtke et al., 2002; Galea et al., 2010). Furthermore, the CWB-SRTT requires cognitive action control, i.e. selection of executing limb (i.e. left or right leg), postural control, and rapid shifting of attentional resources, because participants have to step in one of four directions (front left, front right, back left, or back right) as well as maintain proper motor control. Thus, we hypothesized that greater cognitive demands for the CWB-SRTT would induce functional changes in the lateral PFC since the lateral PFC also plays an important role in cognitive action control and coordinating behavior (Cieslik et al., 2013). Therefore, we selected the lateral PFC as region of interest (ROI) and performed a seed-based rs-FC analysis (Biswal et al., 1995). Then, we investigated the relationship between learning-induced changes in rs-FC and anatomical micro-structures measured before the sensorimotor task. To evaluate white matter structure, we utilized both a newly developed fixel-based analysis (FBA) (Raffelt et al., 2015, 2017) and tract-based spatial statistics (TBSS) focusing on fractional anisotropy (FA) in underlying white matter fibres (Smith et al., 2006). To assess GMV, we conducted a voxel-based morphometry (VBM) analysis (Ashburner and Friston, 2000). Recent studies suggested that short-term motor practice of less than 2 h may induce structural changes in white and gray matter (Sagi et al., 2012; Taubert et al., 2016). Therefore, we also investigated whether structural changes induced by the CWB-SRTT could be observed and furthermore, if the possibly identified changes could be associated with changes in rs-FC of selected brain areas.

2. Material and methods

2.1. Participants

Forty-three healthy right-handed volunteers participated in this study. They were recruited by means of public advertisement and the local Max-Planck Institute participant database. Participants were randomly assigned to a sequence group (SG, 21 participants, 10 females, mean ± SD: 26 ± 3 years old) or control group (CG, 22 participants, 10 females, mean ± SD: 27 ± 5 years old). The study was approved by the local ethics-committee of the University of Leipzig. All participants gave their written informed consent to partake in the experiments according to the Declaration of Helsinki and were remunerated for participation. Data, in anonymous format (according to data protection policy in the ethics agreement) is available on reasonable request.

2.2. Experimental procedure

Participants conducted a CWB-SRTT on 2 consecutive days with measurements of one participant being performed at similar day times. The experiments were conducted from 8 a.m. to 4 p.m. We acquired MRI scans, including resting state functional images, T1-weighted images and diffusion weighted images (DWI), before the CWB-SRTT on day 1 and after the CWB-SRTT on day 2 (Fig. 1A). Participants of the SG completed 20 sequence blocks and one random block before and after all sequence blocks on each day (Fig. 1B). Participants of the CG completed 22 random blocks on each day. The CWB-SRTT lasted approximately 19 min, including 25-s inter-block interval. On day 2, the MRI scan was started immediately after finishing the CWB-SRTT (less than 10 min). After the MRI scan on day 2, participants were asked to recall as many elements of the repeated sequence as possible from their memory according to a forced-choice based questionnaire regarding the presence of a specific sequence (i.e. Yes/No). The parameter of correct recalls was based on the number of correctly recalled consecutive items of the learning sequence.

2.3. Sensorimotor task: complex whole-body serial reaction time task

We used a four-directional CWB-SRTT for the lower extremities. A target cue, displayed on any one of four squares on a monitor, indicated the plate to be stepped on (Fig. 1C). Each square corresponded to one of four custom made plates (150 mm × 200 mm). The distances in the lateral direction of the plates were 0.6 m and the longitudinal distances were 0.5 m. When a target cue appeared, participants were instructed to step on the target plate as quickly as possible. Participants were instructed to use their left foot for all left-side plates and their right foot for all right-side plates (Fig. 1D). For the initial position of the CWB-SRTT, participants were instructed to stand on the two center plates (0.3 m center-to-center plate distance) and were instructed to always revert to this initial position after each motor response. Each following target cue appeared 500 ms after returning to the initial position. If participants made an incorrect response, the target cue remained visible until the correct response was performed. Regarding the presented target cues, we chose 12 items per trial for reasons of comparability, as previous studies have also chosen 12 items during SRTT (e.g. Roberts, 2007; Tzvi et al., 2016). During the sequence block, the target cue appeared in the following order 2-3-2-4-1-3-1-4-3-4-2-1 (1: front left; 2: front right; 3: back left; 4: back right). We did not tell participants about the presence of any sequence making this an implicit sensorimotor learning task. We used a fixed sequence for all SG participants. In the CG, the target cue appeared pseudo randomly with equal probabilities regarding each number. Please note that we determined a limit of maximally three consecutive repetitions per item. All participants were naïve regarding the learning sequence. The CWB-SRTT operated under a custom-made script (C#, Microsoft Visual Studio 2017).

2.4. MRI data acquisition

Participants were scanned on a 3-Tesla Siemens Magnetom PrismaFit scanner using a 32-channel head coil. Blood oxygenation level dependent contrast functional images during resting state were acquired using multiband T2*-weighted echo planar imaging (EPI) free induction decay sequences with the following parameters: field of view (FOV): 204 × 204

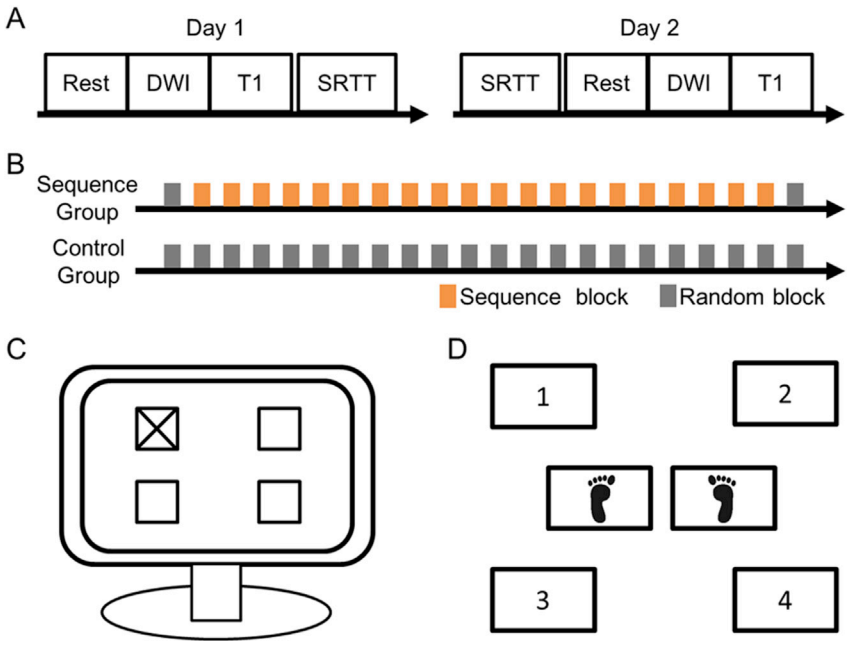

Fig. 1. Experimental settings. (A): A complex whole-body serial reaction time task (CWB-SRTT) was conducted on two consecutive days. Before and after the CWB-SRTT, resting state functional images (Rest), diffusion weighted images (DWI) and T1 weighted images (T1) were acquired. (B): In the sequence group, twenty sequence blocks and two random blocks were performed on each day. In the control group, twenty-two random blocks were performed. (C): Configuration of visual stimuli of the CWB-SRTT. (D): Configuration of contact plates of the CWB-SRTT. Participants stood on middle two plates (i.e. initial position). Participants were asked to respond as quickly as possible using their left foot for the left plates and using their right foot for the right plates. Then, participants returned to the initial position. In the sequence block, the target cue always appeared in the following order (2-3-2-4-1-3-1-4-3-4-2-1).

mm; voxel size: 2.5 mm isotropic with 0.25 mm gap; repetition time (TR): 2000 ms; echo time (TE): 22 ms; and flip angle: 80° (Xu et al., 2013). All participants were asked to close their eyes and not to think about anything during the scan. The acquisition time for the functional scan was 15 min.

Whole brain DWI was acquired with a double spin echo sequence (60 directions; b-value 1000 s/mm^2; 88 slices; FOV: 220 × 220 mm; voxel size: 1.7 mm isotropic, no gap; TR: 5200 ms; TE: 75 ms; flip angle: 90°; GRAPPA acceleration factor = 2) using a multiband acceleration factor of 2 (Setsompop et al., 2012). Seven volumes without diffusion weighting (b = 0 s/mm^2) were acquired, one at the beginning of the sequence and after each block of 10 diffusion weighted images. The acquisition time for the diffusion scan was approximately 10 min.

T1-weighted images were acquired using a MPRAGE (magnetization-prepared rapid acquisition gradient echo) sequence (176 sagittal slices; FOV: 240 × 256 mm; voxel size: 1.0 mm isotropic; TR: 2300 ms; TE: 2.98 ms; inversion time (TI): 900 ms; flip angle: 9°) (Jack et al., 2008). The acquisition time for the structural scan was approximately 9 min, resulting in a total scan time of 34 min.

2.5. Behavioral analysis

We evaluated two distinct response times (i.e. reaction and movement times). Reaction time was defined by the time difference between visual stimulus onset and lifting of the response foot from one of the middle plates. Movement time was defined by the time difference between lifting of the response foot from the middle plate and contact on one of the target plates. Signals were recorded at a sampling rate of 1000 Hz. We calculated the median of reaction and movement times blockwise for each participant. We did not evaluate the accuracy of CWB-SRTT because the number of errors was zero for most participants.

The sequence specific improvements in reaction and movement times were evaluated by calculating time differences between the last random and the last sequence blocks on day 2, respectively. For the CG, time differences between the last two random blocks on day 2 were evaluated. Subsequently, we compared both quantities using two-sample t-tests. To assess whether the sequence specific improvement was associated with the number of recalled items, we calculated Spearman's rank correlation coefficient between the sequence specific improvements and the number of correctly recalled sequence elements.

To evaluate the non-sequence specific improvements in reaction and movement times, we calculated time difference between the first random block on day 1 and the last random block on day 2. Then, we compared them using a two-sample *t*-test, respectively. We also evaluated their improvements within each training day separately.

To check whether initial performance was comparable between two groups, we compared reaction and movement times at the first random block on day 1 using a two-sample *t*-test, respectively.

To assess the degree of retention of sequence specific improvement in the SG, we compared reaction and movement times at the first random and the first sequence block on day 2 using a one-sample *t*-test, respectively.

2.6. Functional image processing

We performed a seed (ROI)-based analysis to evaluate rs-FC using CONN toolbox (Functional Connectivity Toolbox, v.17.f., Neuroimaging Informatics Tools and Resources Clearinghouse, USA, https://www.nitrc.org/projects/conn) implanted in SPM12 (v.7219, Wellcome Trust Center for Neuroimaging, University College London, London, UK, https://www.fil.ion.ucl.ac.uk/spm/software/spm12/) running on MATLAB (v. R2016a, The MathWorks Inc., Natick, USA). EPI images were processed by using the default preprocessing pipeline (realignment, normalization, segmentation, outlier detection, and smoothing with full width at half maximum (FWHM) of 8 mm). Hereafter, denoising was performed using a component-based noise correction method, motion regression, and applying bandpass filtering (0.008–0.09 Hz) (Whitfield-Gabrieli and Nieto-Castanon, 2012). Previous studies involving neuroimaging, non-invasive brain stimulation, and patients with brain lesions suggest that lateral PFC plays a substantial role in sequence learning (Gómez Beldarrain et al., 1999; Robertson et al., 2001; Schmidtke et al., 2002; Schendan et al., 2003; Galea et al., 2010). Therefore, we used the right and left lateral PFC for seed-based analysis. These ROI (i.e. middle frontal gyrus) are defined in CONN toolbox which was made based on the FSL Harvard-Oxford Atlas as a typical anatomical region (https://fsl.fmrib.ox.ac.uk/fsl/fslwiki/Atlases).

To evaluate whether changes in rs-FC after CWB-SRTT were different between two groups, we performed a two-way analysis of variance (ANOVA) with factors time and group. The threshold was set at a voxel level to $p < 0.001$ (uncorrected) to generate the cluster images. Then, we

set the threshold at $p < 0.025$ for the cluster level after FWE correction for multiple comparisons. In addition, we extracted eigenvariates and calculated correlation coefficients between changes in rs-FC and sequence specific improvements of reaction times in the SG. The eigenvariates were extracted from bilateral striatum with a 5 mm sphere centered at −20, 2, 18 and 20, 2, −2 (x, y, z, MNI-coordinates) (please see results).

2.7. Diffusion image processing

We analyzed diffusion data using FBA (Raffelt et al., 2017) and TBSS (Smith et al., 2006). Preprocessing was performed using FSL (v.5.0.9, FMRIB Software Library) (Jenkinson et al., 2012) and MRtrix3 (v.3.0_RC3, http://www.mrtrix.org/). For both analyses, denoising was conducted to improve signal-to-noise-ratio using MRtrix3 (Veraart et al., 2016). Then, distortions, eddy currents and small head movements were corrected using FSL-tools (Andersson et al., 2003; Andersson and Sotiropoulos, 2016). Non-brain tissue was removed using the brain extraction tool (Smith, 2002).

For FBA, a bias field correction and a global intensity normalization on all subjects within our study (using a group-wise registration and the median $b = 0$ white matter value as the reference) were performed (Raffelt et al., 2012). Then, a group-average white matter response function was computed for subsequent analyses. DWI data was upsampled to a voxel size of 1.3 mm (isotropical) as this has been shown to improve anatomical details (Dyrby et al., 2014). The fibre orientation distribution functions (FOD) were calculated using constrained spherical deconvolution (CSD) and maximum spherical harmonics order of 8. To create a study specific FOD template, we used all FOD images from the MRI scan on day 1. Spatial correspondence was obtained by registering all FODs to the FOD template. Then, FODs in the template space were segmented to estimate fibre density (FD), fibre-bundle cross-section (FC) and a combination of both fibre density and fibre-bundle cross-section (FDC). An analysis mask was created by applying a threshold of 0.25 on the average FOD amplitude. Lastly, FC was log-transformed prior to statistical analysis.

To evaluate interaction effects (time x group) for FD, FC and FDC, difference images were computed within-subject. Two-sample t-tests were used to test whether the difference images differed between the two groups. To obtain correlated regions with changes in rs-FC, we conducted correlation analysis for changes in rs-FC between right lateral PFC and left striatum (see results) and FD, FC or FDC. These analyses were performed using connectivity-based fixel enhancement with 5000 permutations (Raffelt et al., 2015). Age and gender were used as covariates of no interest. The statistical threshold was set to $p < 0.05$, after FWE correction for multiple comparisons. To compare results of FBA and TBSS, voxels including significant fixels in our study specific space were transformed into MNI space.

For TBSS analysis, local fitting of voxel-wise diffusion tensors was performed using the FMRIB Diffusion Toolbox, resulting in individual FA maps. All subjects' FA data were transformed into $1 \times 1 \times 1$ mm MNI standard space. In a next step, the mean FA image was created and thresholded at 0.2 to generate a mean FA skeleton representing the centers of all tracts common to the sample. Each subject's aligned FA data was then projected onto this skeleton. To evaluate interaction effects (time x group), difference images within-subject were computed and a two-sample *t*-test was used to test whether the difference images differed between the two groups. To obtain correlated regions with changes in rs-FC, we conducted correlation analyses between FA and changes in rs-FC between right lateral PFC and left striatum (see results). The resulting data was fed into voxelwise statistics based on a non-parametric permutation testing approach using threshold-free cluster enhancement (5000 permutations) (Smith and Nichols, 2009). Age and gender were used as covariates of no interest. The statistical threshold at a voxel-level was set to $p < 0.05$ after FWE correction for multiple comparisons.

2.8. T1 image processing

We performed a VBM analysis using CAT12 (v.1278, Computational Anatomy Toolbox, Jena University Hospital, Departments of Psychiatry and Neurology, Germany; http://www.neuro.uni-jena.de/cat/), a toolbox for SPM12 running under MATLAB. T1-weighted images were modulated and normalized to the MNI standard space and segmented into gray matter, white matter and cerebrospinal fluid using the default approach of combined affine and non-linear registration. Then, the segmented gray matter maps were smoothed with a Gaussian kernel of 8 mm FWHM.

To investigate changes in gray matter volume, we performed a two-way ANOVA with factors *time* and *group*. In addition, we calculated the correlation between GMV before the task and changes in rs-FC. Total intracranial volume, age and gender were included as covariates of no interest in our statistical models. The threshold was set at a voxel level to $p < 0.001$ (uncorrected) to generate the cluster images. Lastly, we set the threshold at $p < 0.05$ for the cluster level after FWE correction for multiple comparisons.

2.9. Time of day effects

Previous studies suggested that the timing of measurement (i.e. time of day) might affect functional and structural results as well as the amount of plasticity (e.g. Sale et al., 2007; Thomas et al., 2018). To check whether the timing of sensorimotor learning or of MRI measurements affected our findings, the main findings such as sequence specific improvements in reaction times, changes in rs-FC between the right lateral PFC and the left striatum, and FC in the right anterior corona radiata measured before the task (please see results) in the SG were compared between AM participants (i.e. 8 a.m. - noon) and PM participants (i.e. noon - 4 p.m.) using a two-sample *t*-test, respectively.

3. Results

3.1. Behavioral data

Initial performance of reaction and movement times did not differ between two groups (reaction time: $t_{(41)} = 0.71$, $p = 0.48$, $d = 0.21$; movement time: $t_{(41)} = 0.15$, $p = 0.88$, $d = 0.05$), indicating that the effect of selection bias was negated. Reaction times improved across sequence blocks in the SG (Fig. 2A). Sequence specific improvements in reaction times were significantly greater than the improvements in reaction times observed in the CG ($t_{(41)} = 4.89$, $p = 1.59 \times 10^{-5}$, $d = 1.48$) (Fig. 2B). All participants in the SG noticed the presence of a specific sequence during the experiment, and the number of correct recalls assessed after the experiment (mean ± SD: 6.2 ± 4.3) was correlated positively with the sequence specific improvements in reaction times ($rho = 0.66$, $p = 0.0011$). Overall, non-sequence specific improvements in reaction times did not reach significance when comparing both groups ($t_{(41)} = 1.89$, $p = 0.07$, $d = 0.57$). When we calculated non-sequence improvements in reaction times within each training day, both groups improved on day 1 ($t_{(20)} = 3.70$, $p = 0.001$, $d = 0.84$; $t_{(21)} = 2.06$, $p = 0.05$, $d = 0.50$, respectively), but not on day 2 ($t_{(20)} = 0.17$, $p = 0.87$, $d = 0.04$; $t_{(21)} = 1.22$, $p = 0.23$, $d = 0.22$, respectively). The sequence specific improvements in reaction times were not correlated with non-sequence specific improvements in the SG ($r = -0.42$, $p = 0.06$). Movement times slightly improved across blocks in both groups (Fig. 2C). Overall, non-sequence specific improvements in movement times did not differ between our two groups ($t_{(41)} = 0.07$, $p = 0.95$, $d = 0.02$). When we calculated non-sequence improvements in movement times within each training day, both groups improved on day 1 ($t_{(20)} = 2.68$, $p = 0.01$, $d = 0.51$; $t_{(21)} = 4.54$, $p = 1.81 \times 10^{-4}$, $d = 0.72$, respectively), but not on day 2 ($t_{(20)} = 1.13$, $p = 0.27$, $d = 0.24$; $t_{(21)} = 1.17$, $p = 0.25$, $d = 0.24$, respectively). Sequence specific improvements in movement times were not observed in the SG. This was not different from the specific

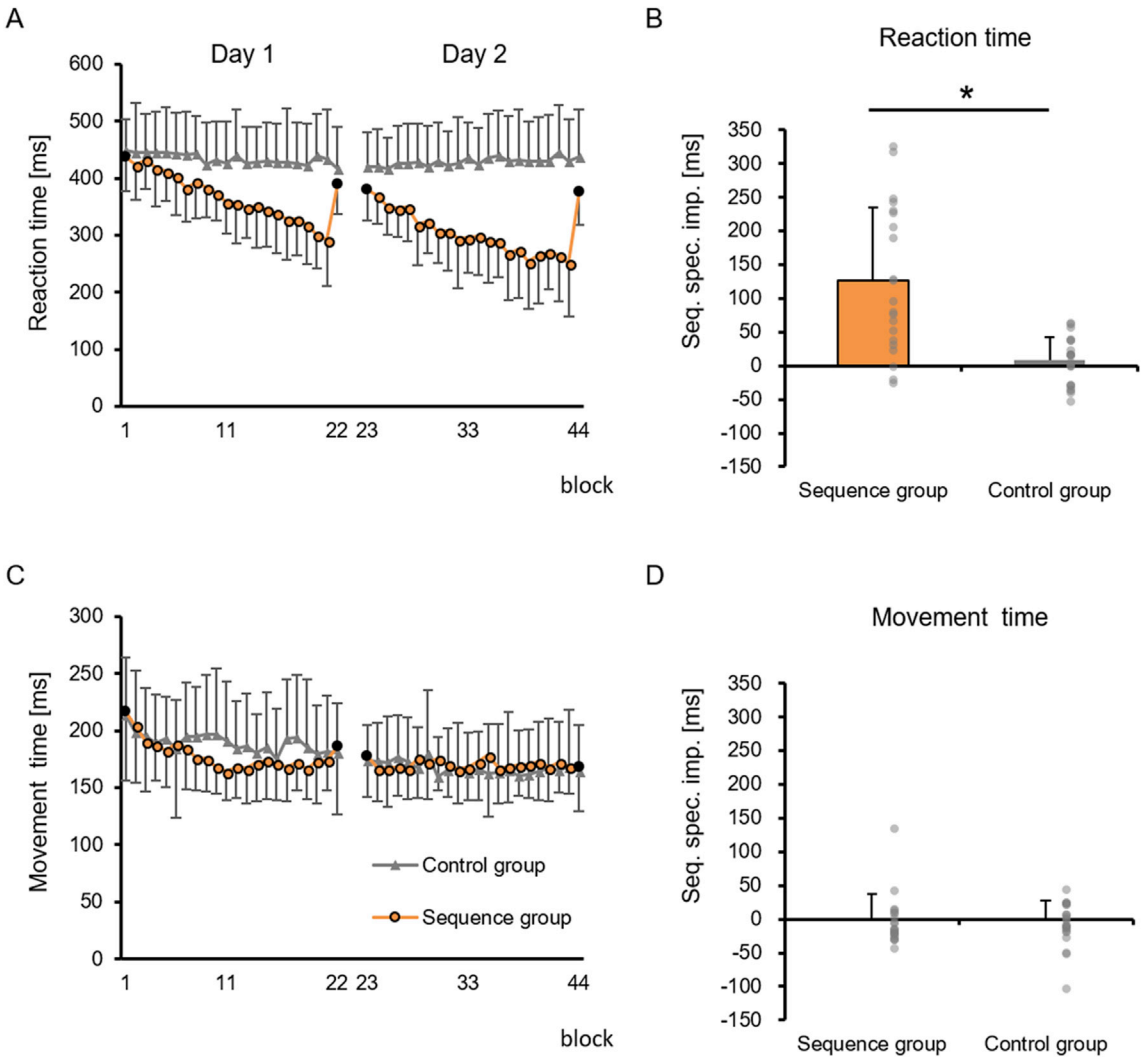

Fig. 2. (A): Reaction times of a whole-body serial reaction time task (CWB-SRTT) in sequence group (SG) and control group (CG). Black circles indicate random blocks in the SG. (B): Sequence specific improvements in reaction times as assessed by difference time between the last random and the last sequence blocks on day 2. Gray plots indicate individual values of each participant. (C): Movement times of the CWB-SRTT in the SG and CG. Black circles indicate random blocks in the SG. (D): Sequence specific improvements in movement times as assessed by difference time between the last random and the last sequence blocks on day 2. Gray plots indicate individual values of each participant. *: $p < 0.001$. Error bars indicate 1 standard deviation.

improvements in movement times in the CG ($t_{(41)} = 0.30$, $p = 0.76$, $d = 0.09$) (Fig. 2D). These results indicate that sensorimotor sequence learning relating to the CWB-SRTT was processed within the cognitive and/or perceptual domain rather than the sensorimotor domain. Some participants in the SG remembered more than six items. However, we did not exclude these participants for later analyses.

Retention or carry-over effects regarding sequence specific improvements did not reach significance in the SG ($t_{(20)} = 1.20$, $p = 0.25$, $d = 0.36$), suggesting that only twenty blocks of sequence on day 1 were not enough to induce significant consolidation/retention of their motor performance.

3.2. Functional data

Seed-based analysis with two-way ANOVA revealed that sensorimotor sequence learning-induced changes in rs-FC between the right lateral PFC and bilateral striatum including caudate nucleus, rostrodorsal and ventral posterior parts of the putamen (peak coordinates: -20, 2, 18 and 20, 2, −2 in MNI-coordinates) were greater in the SG when compared to our CG ($p < 0.025$, FWE corrected) (Fig. 3). However, we did not find any significant interactions using the left lateral PFC ROI. Strength of rs-FC before SRTT on day 1 did not differ between the two groups.

Correlation analysis revealed that changes in rs-FC between the right lateral PFC and the left striatum in the SG were significantly associated with sequence specific improvements in reaction times ($r = 0.53$, $p = 0.014$). However, changes in rs-FC between the right lateral PFC and the right striatum did not reach significance ($r = 0.35$, $p = 0.12$).

Additional correlation analyses, conducted for the purpose of validating the previously mentioned results, showed that changes in rs-FC between right lateral PFC and left/right striatum were not correlated with the degree of retention for sequence specific improvements ($r = 0.11$, $p = 0.63$; $r = 0.07$, $p = 0.76$; respectively) or with initial reaction times at the first random block ($r = -0.12$, $p = 0.61$; $r = 0.23$, $p = 0.31$; respectively).

3.3. Diffusion data

We did not find any main effects or interactions with neither FBA nor TBSS. This indicates that white matter micro-structure did not differ

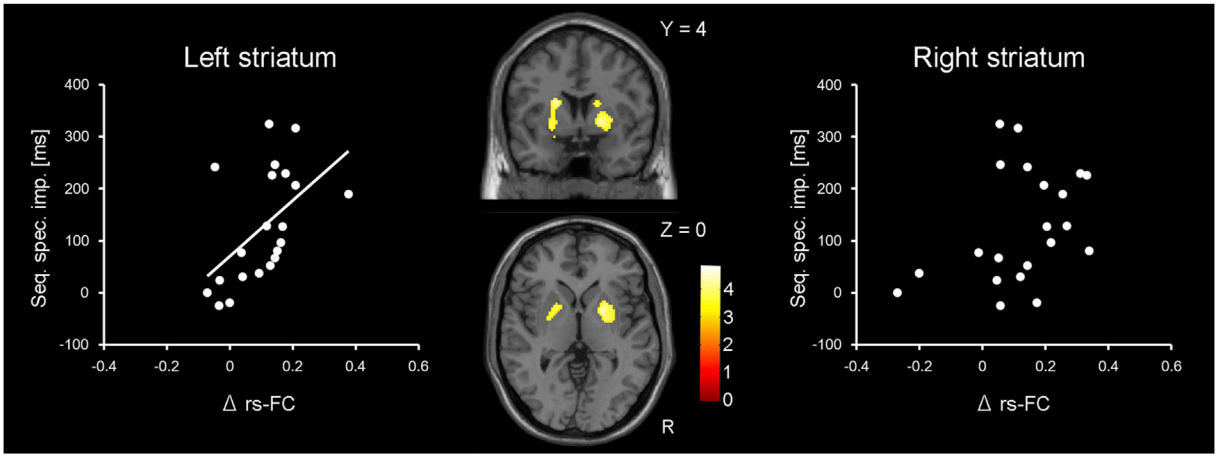

Fig. 3. Results of seed-based analysis for resting state functional images. The seed was the right lateral prefrontal cortex (PFC). Regions in the center images indicate the interacted areas [(sequence group on day 2 > sequence group on day 1) > (control group on day 2 > control group on day 1)]. The threshold was set at voxel level $p < 0.001$ (uncorrected), cluster level $p < 0.025$ (FWE corrected). Side panels show the relationship between sequence specific improvements (Seq. spec. imp.) and changes in resting state functional connectivity (Δ rs-FC) between the right lateral PFC and the left striatum ($r = 0.53$, $p = 0.014$) (left panel) or the right striatum ($r = 0.35$, $p = 0.12$) (right panel) in the sequence group.

between two groups and furthermore, that it does not change during two days of CWB-SRTT. For the SG, FC within the right PFC, as well as FC of transcallosal fibres on scanning day 1 seem to be associated with changes in rs-FC between right middle PFC and left striatum (Fig. 4A and B). Initial FC in the right anterior corona radiata was significantly correlated with the changes in rs-FC ($p < 0.05$, FWE corrected) (Fig. 4C and D). However, we did not find any correlation for FD or FDC. We also failed to observe any correlation between changes in rs-FC and results of FBA in the CG. Using TBSS, we found a negative correlation between FA in the right anterior corona radiata and changes in rs-FC between right lateral PFC and left striatum in the SG (Fig. 4E). The hereby observed significant voxels were almost spatially overlapped with results of FC by means of FBA. We did not find any significant correlation between changes in rs-FC and FA in the CG.

Additionally, we did not find any significant correlation between structural contrast images (post-pre) and changes in rs-FC neither using FBA nor TBSS.

3.4. T1 data

We did not find any main effects or interactions in VBM. This indicated that GMV did not differ between two groups and did not change by two days of CWB-SRTT. In addition, we did not find any correlation between changes in rs-FC and GMV before CWB-SRTT on day 1 or the contrast images (post-pre).

3.5. Time of day effects

We did not find any significant differences between AM and PM participants. This indicated that our results cannot be explained by the timing of sensorimotor learning or of MRI measurements.

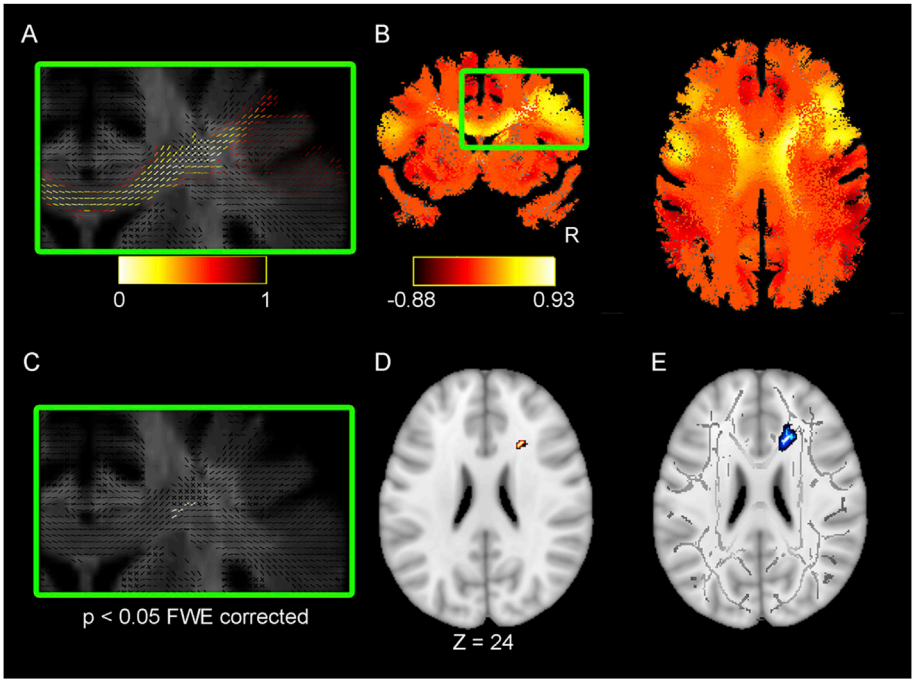

Fig. 4. (A): For visualization, p-values (FWE corrected) for fixel of fibre-bundle cross-section (FC) in association with changes in resting state functional connectivity (rs-FC) between the right lateral prefrontal cortex (PFC) and left striatum was rendered for a study-specific fixel template. (B): Effect size of FC in association with changes in rs-FC between the right lateral prefrontal cortex (PFC) and left striatum was rendered for a study-specific tractogram. (C): Significant fixels of FC in association with change in rs-FC between the right lateral PFC and left striatum in the sequence group (SG) ($p < 0.05$, FWE corrected). (D): Significant positive correlation between FC in the right anterior corona radiata and changes in rs-FC between the right lateral PFC and left striatum in the SG ($p < 0.05$, FWE corrected). Significant cluster in a study-specific template was transformed into the MNI space. (E): Significant negative correlation between FA in the right anterior corona radiata and changes in rs-FC between right lateral PFC and left striatum in the SG ($p < 0.05$, FWE corrected).

4. Discussion

Here, we show for the first time that short-term learning of a complex movement pattern by means of CWB-SRTT is associated with distinct changes in rs-FC between right lateral PFC and bilateral striatum. Even more interesting, sequence-specific improvements were significantly correlated with learning-induced changes between right lateral PFC and left striatum. Furthermore, these rs-FC changes were correlated with initial FC located within the same anatomical area.

Sequence specific improvements were observed in reaction times, yet not for movement times, suggesting that sequence learning occurred within the cognitive and/or perceptual domain rather than the motor domain. Indeed, sequence specific improvements were correlated with the number of correct sequence-recalls. Therefore, remembered sequence items potentially contributed to sequence specific improvements in some participants. Since participants in the CG completed a similar whole-body movement task without following any specific sequence, changes in rs-FC between right lateral PFC and striatum observed in the SG are likely associated with the acquisition of sequence rather than exercise itself or non-sequence specific performance improvements.

Previous studies demonstrated that the lateral PFC plays an important role in sensorimotor sequence learning, especially during its early stages (Jenkins et al., 1994; Dayan and Cohen, 2011). In addition, during the early sensorimotor learning phase of a sequential finger tapping task, functional connectivity between frontal areas including the lateral PFC and caudate nucleus increased in association with a decrease in performance variability following short-term (about 10 min) sensorimotor sequence learning (Albouy et al., 2012). These findings imply that sensorimotor sequence memory is stored in the "associative" circuit during early learning phase (Hikosaka et al., 2002; Penhune and Steele, 2012). Therefore, our finding that increases in rs-FC between the lateral PFC and associative striatum were correlated with sequence specific improvements, is consistent with previous findings. Additional histological support for this assumption was provided by Fallon and Ziegler (1979) and Innocenti and colleagues (2017) as they were able to show that the lateral PFC was directly connected to the contralateral caudate nucleus and putamen. Sami and colleagues demonstrated that, immediately after an explicit SRTT, strength of the resting state executive fronto-cerebellar network increased, whereas strength of the resting state sensorimotor network remained unchanged (Sami et al., 2014). However, 6 h after termination of motor practice, strength of the executive fronto-cerebellar network decreased, and strength of the sensorimotor network significantly increased (Sami et al., 2014). Since they evaluated the changes in rs-FC within intrinsic networks as identified by independent components analysis, seed-based analysis conducted in this study provides new evidence. That is, we show that rs-FC changes also occur between distinct networks involving the lateral PFC and sensorimotor striatum. This might indicate a memory transfer from the cognitive/executive network to the sensorimotor network after complex whole-body sequence learning. An association between right dominance in lateral PFC and sensorimotor sequence memory was reported by previous studies using positron emission tomography and a virtual lesion technique induced by transcranial magnetic stimulation (TMS) (Jenkins et al., 1994; Galea et al., 2010). Therefore, our finding of right PFC dominance is also consistent with this previous investigation.

We found a positive correlation in FC, as well as a negative correlation in FA with changes in rs-FC. The negative correlation in FA is consistent with a previous study demonstrating that offline gains following sensorimotor sequence learning were associated with smaller FA in the right anterior corona radiata (Vien et al., 2016). Previous studies suggested that the parameter of FA is influenced by several factors such as axon diameter, inter-axon spacing, membrane permeability, myelination, and coherence of axon orientations (Beaulieu, 2002; Raffelt et al., 2012). For example, a voxel containing crossing fibres might have smaller FA as compared to a voxel without crossing fibres (Raffelt et al., 2012). On the other hand, FC is a more tangible index of white matter structure because during FBA, FC is evaluated in each fibre element (i.e. fixel) within a voxel (Raffelt et al., 2015, 2017). Indeed, significant fixels in the right anterior corona radiata were observed in voxels which naturally contain crossing fibres (Fig. 4C). Therefore, we consider smaller FA in the right anterior corona radiata to be at least partially explained by greater FC of crossing fibres. However, in the present study, we were not able to determine which microstructural factor induced the difference between FA and FC values. Future studies including histological assessment are needed to clarify this limitation. GMV was not associated with changes in rs-FC. Therefore, these results indicate that learning-induced changes in rs-FC observed following a CWB-SRTT are associated with the individual micro-structural makeup of white matter connections within right lateral PFC. To the best of our knowledge, the present study is the first to present the relationship between sensorimotor sequence learning-induced changes in rs-FC and FC of underlying fibre connections.

Previous studies investigating motor learning demonstrated that functional and structural changes occurred in motor-related regions such as M1 (Dayan and Cohen, 2011; Taubert et al., 2016). However, in an additional analysis using M1 ROIs, we did not find functional or structural changes. We speculate that this contradiction could be explained by the amount of training sessions. That is, behavioral results revealed no sequence specific improvements in movement times after two days of CWB-SRTT. Furthermore, reaction times in the SG gradually improved, and failed to reach a plateau on both training days, indicating that participants remained in the early phase of sensorimotor sequence learning even on day 2. Therefore, we speculate that extensive motor practice of CWB-SRTT might induce functional and structural changes involving M1 since it has been shown that activity in M1 increases especially in the later phase of motor learning (Dayan and Cohen, 2011). Nevertheless, here we propose the usage of a novel CWB-SRTT in order to investigate sensorimotor sequence learning-induced functional and structural changes as it reflects the demands of natural movements more realistically opposed to the traditional SRTT.

As a limitation of our study, it must be noted that we only measured functional images before CWB-SRTT on day 1 and after CWB-SRTT on day 2. Therefore, changes in rs-FC might reflect both offline effects on day 2 and consolidation effects originating from day 1. However, behavioral results show that retention of sequence specific sensorimotor skill does not reach significance. In addition, control correlation analyses revealed that changes in rs-FC do not correlate with the degree of retention. Therefore, we conclude that the observed changes in rs-FC presumably reflect offline effects on day 2 rather than consolidation. Due to the nature of our task we were not able to dissociate implicit and explicit learning components. This is an inherent problem to sequence-learning tasks (Robertson, 2007). That is, some participants notice the presence of a fixed sequence, but others do not, even if the same implicit task is performed (Sami et al., 2014; Tzvi et al., 2016). A previous study demonstrated that the lateral PFC was activated during both implicit and explicit SRTT (Schendan et al., 2003), while other studies suggested that implicit and explicit learning is associated with different neural substrates/mechanisms (Lang et al., 2006; Darsaud et al., 2011; Hardwick et al., 2012; Yordanova et al., 2015; Tzvi et al., 2016). In the present study, participants noticed the presence of a fixed sequence during the experiment and were able to recall several items after the experiment. In addition, the number of correct recalls was significantly correlated with the sequence specific improvements in reaction times. Therefore, it was possible that this knowledge gain towards the end of the task might have influenced changes in functional connectivity. Unfortunately, using our task, it is virtually impossible to disentangle implicit from explicit components of learning and how this influences learning-dependent neuroplasticity. Future studies are needed to determine the relationship between implicit/explicit sensorimotor memory and functional/structural connectivity involving the lateral PFC. The association between changes in rs-FC and behavioral performance improvements serves as an indication regarding right lateral PFC contribution concerning this matter. Future studies could use non-invasive brain stimulation techniques

such as TMS to the right lateral PFC to investigate the causal relationship behind our finding. In the present study, we focused on the lateral PFC because previous studies suggested that both implicit and explicit learning components are associated with the lateral PFC (Schendan et al., 2003; Gómez Beldarrain et al., 1999; Robertson et al., 2001; Schmidtke et al., 2002; Galea et al., 2010). However, functional and/or structural connectivity between other regions might also be related to sensorimotor sequence learning of the CWB-SRTT.

In conclusion, sensorimotor sequence learning of a CWB-SRTT increased rs-FC between the right lateral PFC and striatum. This increase was positively correlated with FC within the right lateral PFC. Therefore, learning-induced changes in rs-FC were associated with the micro-structural makeup of white matter connections beneath related regions. Such multi-modal brain assessments, as well as the application of a CWB-SRTT improve our understanding regarding underlying neural mechanisms of sensorimotor sequence learning in an integrated and a more realistic way than traditional hand SRTTs. These insights might be useful for a number of applied fields including neural rehabilitation and sports neuroscience in order to further develop effective treatment and training methods.

Declaration of interest

None.

Acknowledgments

This work was supported by JSPS KAKENHI Grant Number JP16J01324 to NM and the Max-Planck Society. All authors declare no conflicts of interest.

References

Albouy, G., Sterpenich, V., Vandewalle, G., Darsaud, A., Gais, S., Rauchs, G., Desseilles, M., Boly, M., Dang-Vu, T., Balteau, E., Degueldre, C., Phillips, C., Luxen, A., Maquet, P., 2012. Neural correlates of performance variability during motor sequence acquisition. Neuroimage 60, 324–331.

Andersson, J.L., Skare, S., Ashburner, J., 2003. How to correct susceptibility distortions in spin-echo echo-planar images: application to diffusion tensor imaging. Neuroimage 20, 870–888.

Andersson, J.L.R., Sotiropoulos, S.N., 2016. An integrated approach to correction for off-resonance effects and subject movement in diffusion MR imaging. Neuroimage 125, 1063–1078.

Ashburner, J., Friston, K.J., 2000. Voxel-based morphometry–the methods. Neuroimage 11, 805–821.

Beaulieu, C., 2002. The basis of anisotropic water diffusion in the nervous system - a technical review. NMR Biomed. 15, 435–455.

Betzel, R.F., Byrge, L., He, Y., Goñi, J., Zuo, X.N., Sporns, O., 2014. Changes in structural and functional connectivity among resting-state networks across the human lifespan. Neuroimage 102, 345–357.

Biswal, B., Yetkin, F.Z., Haughton, V.M., Hyde, J.S., 1995. Functional connectivity in the motor cortex of resting human brain using echo-planar MRI. Magn. Reson. Med. 34, 537–541.

Cieslik, E.C., Zilles, K., Caspers, S., Roski, C., Kellermann, T.S., Jakobs, O., Langner, R., Laird, A.R., Fox, P.T., Eickhoff, S.B., 2013. Is there "one" DLPFC in cognitive action control? Evidence for heterogeneity from co-activation-based parcellation. Cerebr. Cortex 23, 2677–2689.

Darsaud, A., Wagner, U., Balteau, E., Desseilles, M., Sterpenich, V., Vandewalle, G., Albouy, G., Dang-Vu, T., Collette, F., Boly, M., Schabus, M., Degueldre, C., Luxen, A., Maquet, P., 2011. Neural precursors of delayed insight. J. Cogn. Neurosci. 23, 1900–1910.

Dayan, E., Cohen, L.G., 2011. Neuroplasticity subserving motor skill learning. Neuron 72, 443–454.

Dyrby, T.B., Lundell, H., Burke, M.W., Reislev, N.L., Paulson, O.B., Ptito, M., Siebner, H.R., 2014. Interpolation of diffusion weighted imaging datasets. Neuroimage 103, 202–213.

Fallon, J.H., Ziegler, B.T., 1979. The crossed cortico-caudate projection in the rhesus monkey. Neurosci. Lett. 15, 29–32.

Galea, J.M., Albert, N.B., Ditye, T., Miall, R.C., 2010. Disruption of the dorsolateral prefrontal cortex facilitates the consolidation of procedural skills. J. Cogn. Neurosci. 22, 1158–1164.

Gómez Beldarrain, M., Grafman, J., Pascual-Leone, A., Garcia-Monco, J.C., 1999. Procedural learning is impaired in patients with prefrontal lesions. Neurology 52, 1853–1860.

Hardwick, R.M., Rottschy, C., Miall, R.C., Eickhoff, S.B., 2012. A quantitative meta-analysis and review of motor learning in the human brain. Neuroimage 67, 283–297.

Hikosaka, O., Nakamura, K., Sakai, K., Nakahara, H., 2002. Central mechanisms of motor skill learning. Curr. Opin. Neurobiol. 12, 217–222.

Innocenti, G.M., Dyrby, T.B., Andersen, K.W., Rouiller, E.M., Caminiti, R., 2017. The crossed projection to the striatum in two species of monkey and in humans: behavioral and evolutionary significance. Cerebr. Cortex 27, 3217–3230.

Jack Jr., C.R., Bernstein, M.A., Fox, N.C., Thompson, P., Alexander, G., Harvey, D., Borowski, B., Britson, P.J., L. Whitwell, J., Ward, C., Dale, A.M., Felmlee, J.P., Gunter, J.L., Hill, D.L., Killiany, R., Schuff, N., Fox-Bosetti, S., Lin, C., Studholme, C., DeCarli, C.S., Krueger, G., Ward, H.A., Metzger, G.J., Scott, K.T., Mallozzi, R., Blezek, D., Levy, J., Debbins, J.P., Fleisher, A.S., Albert, M., Green, R., Bartzokis, G., Glover, G., Mugler, J., Weiner, M.W., 2008. The alzheimer's disease neuroimaging initiative (ADNI): MRI methods. J. Magn. Reson. Imaging 27, 685–691.

Jenkins, I.H., Brooks, D.J., Nixon, P.D., Frackowiak, R.S., Passingham, R.E., 1994. Motor sequence learning: a study with positron emission tomography. J. Neurosci. 14, 3775–3790.

Jenkinson, M., Beckmann, C.F., Behrens, T.E., Woolrich, M.W., Smith, S.M., 2012. FSL. Neuroimage 62, 782–790.

Lang, S., Kanngieser, N., Jaśkowski, P., Haider, H., Rose, M., Verleger, R., 2006. Precursors of insight in event-related brain potentials. J. Cogn. Neurosci. 18, 2152–2166.

Lehéricy, S., Benali, H., Van de Moortele, P.F., Pélégrini-Issac, M., Waechter, T., Ugurbil, K., Doyon, J., 2005. Distinct basal ganglia territories are engaged in early and advanced motor sequence learning. Proc. Natl. Acad. Sci. U. S. A 102, 12566–12571.

Mizuguchi, N., Katayama, T., Kanosue, K., 2018. The effect of cerebellar transcranial direct current stimulation on a throwing task depends on individual level of task performance. Neuroscience 371, 119–125.

Mizuguchi, N., Nakata, H., Kanosue, K., 2016. Motor imagery beyond the motor repertoire: activity in the primary visual cortex during kinesthetic motor imagery of difficult whole body movements. Neuroscience 315, 104–113.

Mizuguchi, N., Kanosue, K., 2017. Changes in brain activity during action observation and motor imagery: their relationship with motor learning. Prog. Brain Res. 234, 189–204.

Penhune, V.B., Steele, C.J., 2012. Parallel contributions of cerebellar, striatal and M1 mechanisms to motor sequence learning. Behav. Brain Res. 226, 579–591.

Raffelt, D.A., Smith, R.E., Ridgway, G.R., Tournier, J.D., Vaughan, D.N., Rose, S., Henderson, R., Connelly, A., 2015. Connectivity-based fixel enhancement: whole-brain statistical analysis of diffusion MRI measures in the presence of crossing fibres. Neuroimage 117, 40–55.

Raffelt, D., Tournier, J.D., Rose, S., Ridgway, G.R., Henderson, R., Crozier, S., Salvado, O., Connelly, A., 2012. Apparent Fibre Density: a novel measure for the analysis of diffusion-weighted magnetic resonance images. Neuroimage 59, 3976–3994.

Raffelt, D.A., Tournier, J.D., Smith, R.E., Vaughan, D.N., Jackson, G., Ridgway, G.R., Connelly, A., 2017. Investigating white matter fibre density and morphology using fixel-based analysis. Neuroimage 144, 58–73.

Robertson, E.M., 2007. The serial reaction time task: implicit motor skill learning? J. Neurosci. 27, 10073–10075.

Robertson, E.M., Tormos, J.M., Maeda, F., Pascual-Leone, A., 2001. The role of the dorsolateral prefrontal cortex during sequence learning is specific for spatial information. Cerebr. Cortex 11, 628–635.

Ruddy, K.L., Leemans, A., Woolley, D.G., Wenderoth, N., Carson, R.G., 2017. Structural and functional cortical connectivity mediating cross education of motor function. J. Neurosci. 37, 2555–2564.

Sagi, Y., Tavor, I., Hofstetter, S., Tzur-Moryosef, S., Blumenfeld-Katzir, T., Assaf, Y., 2012. Learning in the fast lane: new insights into neuroplasticity. Neuron 73, 1195–1203.

Sale, M.V., Ridding, M.C., Nordstrom, M.A., 2007. Factors influencing the magnitude and reproducibility of corticomotor excitability changes induced by paired associative stimulation. Exp. Brain Res. 181, 615–626.

Sami, S., Robertson, E.M., Miall, R.C., 2014. The time course of task-specific memory consolidation effects in resting state networks. J. Neurosci. 34, 3982–3992.

Schendan, H.E., Searl, M.M., Melrose, R.J., Stern, C.E., 2003. An FMRI study of the role of the medial temporal lobe in implicit and explicit sequence learning. Neuron 37, 1013–1125.

Schmidtke, K., Manner, H., Kaufmann, R., Schmolck, H., 2002. Cognitive procedural learning in patients with fronto-striatal lesions. Learn. Mem. 9, 419–429.

Setsompop, K., Cohen-Adad, J., Gagoski, B.A., Raij, T., Yendiki, A., Keil, B., Wedeen, V.J., Wald, L.L., 2012. Improving diffusion MRI using simultaneous multi-slice echo planar imaging. Neuroimage 63, 569–580.

Smith, S.M., 2002. Fast robust automated brain extraction. Hum. Brain Mapp. 17, 143–155.

Smith, S.M., Jenkinson, M., Johansen-Berg, H., Rueckert, D., Nichols, T.E., Mackay, C.E., Watkins, K.E., Ciccarelli, O., Cader, M.Z., Matthews, P.M., Behrens, T.E., 2006. Tract-based spatial statistics: voxelwise analysis of multi-subject diffusion data. Neuroimage 31, 1487–1505.

Smith, S.M., Nichols, T.E., 2009. Threshold-free cluster enhancement: addressing problems of smoothing, threshold dependence and localisation in cluster inference. Neuroimage 44, 83–98.

Taubert, M., Mehnert, J., Pleger, B., Villringer, A., 2016. Rapid and specific gray matter changes in M1 induced by balance training. Neuroimage 133, 399–407.

Thomas, C., Sadeghi, N., Nayak, A., Trefler, A., Sarlls, J., Baker, C.I., Pierpaoli, C., 2018. Impact of time-of-day on diffusivity measures of brain tissue derived from diffusion tensor imaging. Neuroimage 173, 25–34.

Tzvi, E., Verleger, R., Münte, T.F., Krämer, U.M., 2016. Reduced alpha-gamma phase amplitude coupling over right parietal cortex is associated with implicit visuomotor sequence learning. Neuroimage 141, 60–70.

Veraart, J., Novikov, D.S., Christiaens, D., Ades-Aron, B., Sijbers, J., Fieremans, E., 2016. Denoising of diffusion MRI using random matrix theory. Neuroimage 142, 394–406.
Vien, C., Boré, A., Lungu, O., Benali, H., Carrier, J., Fogel, S., Doyon, J., 2016. Age-related white-matter correlates of motor sequence learning and consolidation. Neurobiol. Aging 48, 13–22.
Whitfield-Gabrieli, S., Nieto-Castanon, A., 2012. Conn: a functional connectivity toolbox for correlated and anticorrelated brain networks. Brain Connect. 2, 125–141.
Xu, J., Moeller, S., Auerbach, E.J., Strupp, J., Smith, S.M., Feinberg, D.A., Yacoub, E., Uğurbil, K., 2013. Evaluation of slice accelerations using multiband echo planar imaging at 3 T. Neuroimage 83, 991–1001.
Yordanova, J., Kirov, R., Kolev, V., 2015. Increased performance variability as a marker of implicit/explicit interactions in knowledge awareness. Front. Psychol. 6, 1957.